

Cite this article as: Zhu Shiqiang, Wang Kehuan, Wei Wenting, et al. Local Hot Gas Forming of Long Axis Bellow with Non-uniform Temperature[J]. Rare Metal Materials and Engineering, 2021, 50(08): 2738-2744.

ARTICLE

# Local Hot Gas Forming of Long Axis Bellow with Non-uniform Temperature

Zhu Shiqiang<sup>1,2,3</sup>, Wang Kehuan<sup>1,2</sup>, Wei Wenting<sup>2</sup>, Liu Gang<sup>1,2</sup>

<sup>1</sup> National Key Laboratory for Precision Hot Processing of Metals, Harbin Institute of Technology, Harbin 150001, China; <sup>2</sup> School of Materials Science and Engineering, Harbin Institute of Technology, Harbin 150001, China; <sup>3</sup> Capital Aerospace Machinery Corporation Limited, Beijing 100076, China

**Abstract:** A novel local hot gas forming (LHGF) process with non-uniform temperature field was proposed to form AZ31 magnesium alloy long axis bellow. Hot uniaxial tensile tests at temperatures ranging from 573 K to 673 K and strain rates ranging from 0.001 s<sup>-1</sup> to 0.1 s<sup>-1</sup> were carried out to study the hot deformation behavior of AZ31 magnesium alloy. Forming apparatuses with independent heating and cooling facilities were developed to achieve the non-uniform temperature field. Local hot gas forming tests of single wave bellow were performed to study the effects of temperature and gas pressure on the forming process and to determine the proper processing windows. A long axis bellow with 5 waves was finally formed to validate the novel process. Results show that the maximum temperature in the cooling zone can be kept below 50 °C and the temperature in the heating zone can be accurately controlled with fluctuation less than ±5 °C. A qualified AZ31 magnesium alloy long axis bellow with 5 waves is formed with small dies at 623 K under a constant gas pressure of 14 MPa. The average grain size at the wave crest is refined from 21.8 μm in the initial to 16.56 μm after forming due to the dynamic recrystallization during the forming.

**Key words:** long axis bellow; hot gas forming; local forming; non-uniform temperature field

Metal bellows are a cylindrical thin-walled shell with radial ripples, which can be extended or shortened under the action of axial tension or compression<sup>[1-3]</sup>. There are different types of bellows with the diameter ranging from millimeters to meters, and the wave number ranging from a few to hundreds, which have been widely used in industries. In order to achieve the lightweight aim, bellows made of lightweight alloys such as magnesium alloys and aluminum alloys become more and more popular<sup>[4]</sup>. However, how to manufacture such lightweight bellows efficiently is a big challenge because of the poor formability of the lightweight alloys.

Hydroforming process is commonly used in the manufacturing of metal bellows<sup>[5-7]</sup>. Lots of researches have been devoted to solve the cracking, wrinkling, bulking or local thinning during the hydroforming of metal bellows<sup>[8,9]</sup>. However, lightweight bellows such as magnesium alloy bellow are very difficult to be formed at room temperature due to the limited ductility. However, hydroforming can only be used at room temperature<sup>[10]</sup>. In order to extend hydroforming to

elevated temperature, hot gas forming is developed<sup>[11]</sup>, where compressed gas is used to replace the liquid water<sup>[12]</sup>. This technology is similar to superplastic forming, where the forming media is also compressed gas. However, the processing windows are very different, and lower temperature, higher strain rate and high pressure are used in hot gas forming to improve the forming efficiency and to reduce the cost<sup>[13]</sup>. This technology has been applied in steels<sup>[14-16]</sup> and aluminum alloys<sup>[17-19]</sup>. However, few researches can be found about hot gas forming of magnesium alloys.

Regarding to forming metal bellows at elevated temperature, a semi-dieless forming process for metal bellows was proposed in Ref. [3], where the bellow was formed by local induction heating and axial compression. During the semi-dieless forming process, the tube was locally heated, and two sides of the hot area were cooled to generate the flow stress difference and to induce buckling at the locally heated area with low flow stress<sup>[3]</sup>. However, it is difficult to control the dimensional accuracy by this process. A Ti31 titanium alloy

Received date: August 11, 2020

Corresponding author: Wang Kehuan, Ph. D., Lecturer, National Key Laboratory for Precision Hot Processing of Metals, Harbin Institute of Technology, Harbin 150001, P. R. China, Tel: 0086-451-86418631, E-mail: wangkehuan@hit.edu.cn

Copyright © 2021, Northwest Institute for Nonferrous Metal Research. Published by Science Press. All rights reserved.

bellow was successfully formed at 700 °C by current-assisted forming technology<sup>[20]</sup>, where Ti31 titanium alloy was heated to 700 °C by current and then formed by gas pressure and axial feeding. However, few researches can be found about the forming of long axis bellows.

A novel local hot gas forming (LHGF) process with non-uniform temperature field was proposed to form AZ31 magnesium alloy long axis bellow. Small forming dies were used to form the bellows step by step, and one wave was formed a time. The forming dies were divided into forming zone and cooling zone, and the formed wave was placed either in cooling zone or in air to prevent the further deformation. A qualified AZ31 magnesium alloy long axis bellow with 5 waves was successfully formed with small dies at 623 K under a constant gas pressure of 14 MPa.

## 1 Experiment

The chemical composition of the AZ31 magnesium alloy used in this study is shown in Table 1. The magnesium alloy tube used for the experiment was a hot extruded seamless tube, with an outer diameter of 44 mm and an average thickness of 2.1 mm.

The tensile tests were conducted on an electronic universal material testing machine (Instron 5500R). The samples were obtained by wire cutting on a magnesium alloy extruded tube, and the tensile direction coincided with the axial direction of the tube. The dimension of the dog-bone shaped tensile sample is shown in Fig.1. Because the samples were cut from a tube, the clamping section needed to be flattened. The tensile tests were carried out at temperatures ranging from 573 K to 673 K with the initial strain rate of 0.001~0.1 s<sup>-1</sup>. The sample was pulled until failure, and then the fractured sample was immediately quenched in water. In order to ensure the repeatability of the results, three groups of tests were conducted for each test condition.

The three-dimensional geometry and dimension of the bellows studied are shown in Fig. 2, in which the tube diameter and the wave height are 44 and 4.2 mm, respectively. The fillet radius of the transition zone is 4 mm, the average thickness of the tube is 2.1 mm, and  $n$  is the wave spacing.

**Table 1** Chemical composition of AZ31 magnesium alloy tube (wt%)

Al	Zn	Mn	Fe	Si	Cu	Ni	Mg
3.05	1.02	0.12	0.001	0.01	0.01	0.01	Bal.

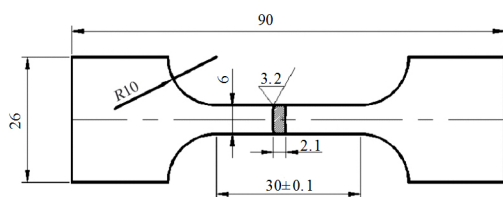


**Fig.1** Dimensions of the AZ31 magnesium alloy samples for hot tensile tests

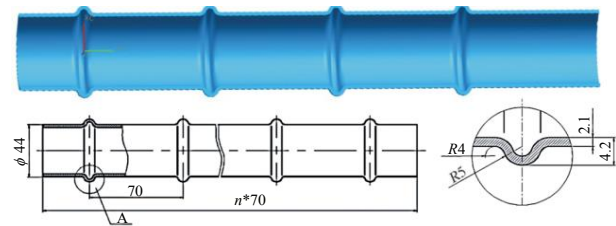


**Fig.2** Three-dimensional geometry and dimension of bellows

The schematic diagram of the forming apparatus is shown in Fig.3. The forming dies consist of cooling zone, heat insulation zone and forming zone. The forming zone was heated to the predetermined temperature by resistance heating rod, and the cooling zone was cooled by water circulation. Insulating asbestos was used to isolate the heat-exchange between the forming zone and the cooling zone to ensure that the temperature of cooling zone is below 50 °C. High temperature seal rings were used to achieve the sealing. The both ends of the tube were connected by a screw and there was an air inlet in the left end. During the forming of the bellows, the forming zone was heated to the targeted temperature. After the temperature was stabilized, the sealed tube was put into the die and soaked for 5 min to stabilize the temperature. Thermocouple was used to measure the temperature of the tube in the forming area. High pressure gas was introduced into the tube according to the loading path and the bulging height of bellows was measured in real time with displacement sensor. The gas pressure was released when the bulging height of the bellows reached 4.2 mm. The formed bellows were taken out and cooled in water immediately to freeze the microstructure.

## 2 Results and Discussion

### 2.1 Hot deformation behavior of AZ31 magnesium alloy

Fig. 4 shows the true stress-strain curves of AZ31 magnesium alloy under different strain rates and temperatures. The flow stress of magnesium alloy increases with increasing the strain rate at a constant temperature. The total elongation of the material changes little with decreasing the strain rate from 0.1 s<sup>-1</sup> to 0.01 s<sup>-1</sup>. Due to the low stacking fault energy, it is not conducive to the occurrence of dynamic recovery in AZ31 magnesium alloy, and dynamic recrystallization (DRX) also does not occur at strain rate of 0.1 and 0.01 s<sup>-1</sup>, so the elongation cannot increase significantly. But with increasing the temperature, DRX occurs at the strain rate of 0.001 s<sup>-1</sup>, which consumes the dislocations and results in larger elongation. Material softening is also observed during the deformation at the strain rate of 0.001 s<sup>-1</sup> due to DRX.

Fig. 5 shows the yield strength and peak stress of AZ31 magnesium alloy under different strain rates and temperatures. It can be seen from Fig. 5a that the yield strength of the material decreases with the increase of temperature. At the strain rate of 0.1 s<sup>-1</sup>, the yield strength decreases from 70.57 MPa at 573 K to 63.82 MPa at 673 K, and at the strain rate of 0.001 s<sup>-1</sup>, the yield strength decreases from 43.70 MPa at 573

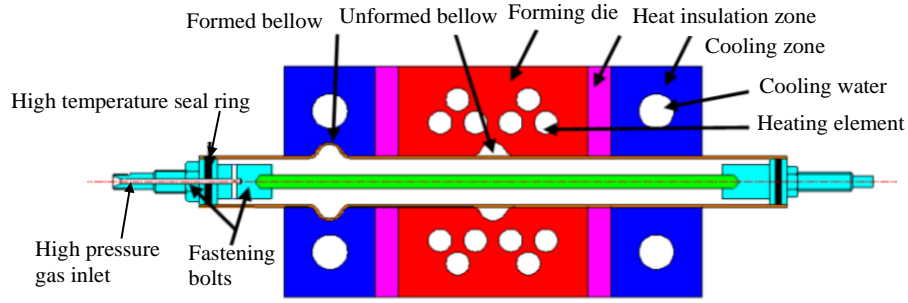


Fig.3 Schematic diagram of the forming apparatus for local hot gas forming with non-uniform temperature field

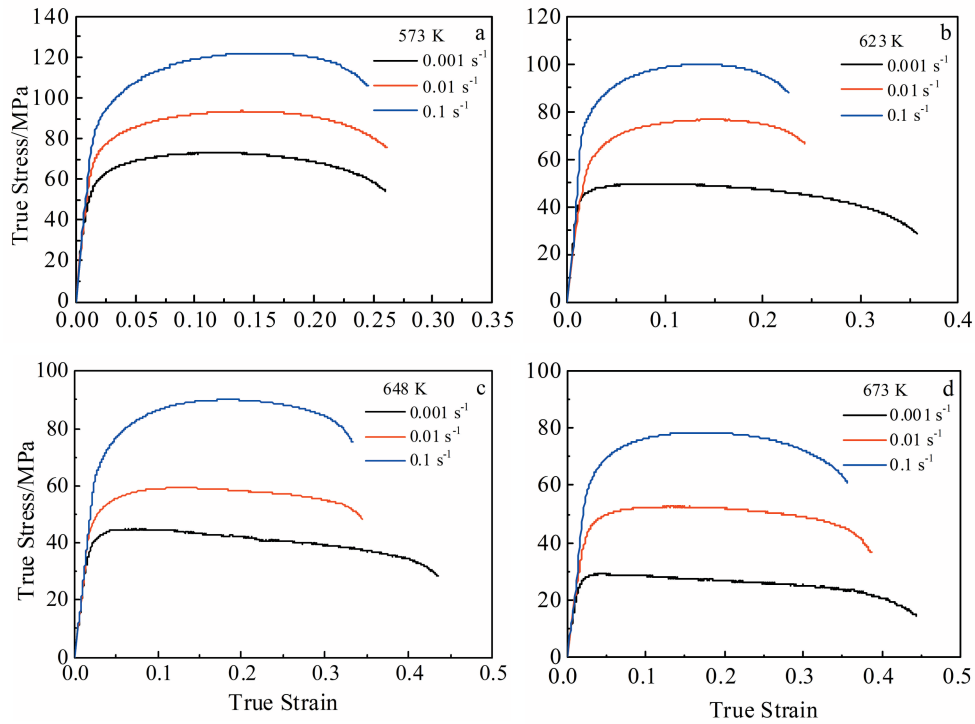


Fig.4 Stress-strain curves of AZ31 magnesium alloy at different strain rates and temperatures: (a) 573 K, (b) 623 K, (c) 648 K, and (d) 673 K

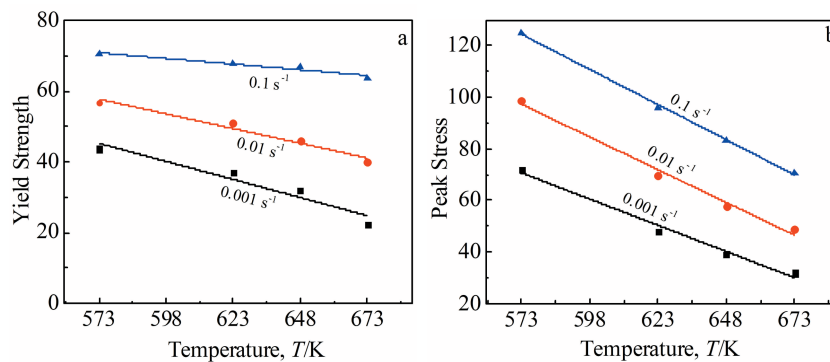


Fig.5 Relevance between yield strength (a), peak stress (b) and temperature of magnesium alloy at different strain rates

K to 22.24 MPa at 673 K. Under different strain rate conditions, the yield strength of materials has different sensitivity to temperature. The lower the strain rate, the higher

the sensitivity of magnesium alloy to temperature. At the same temperature, the yield strength of magnesium alloy decreases with the strain rate. Moreover, the sensitivity of magnesium

alloy to the strain rate increases with the increase of temperature. Fig. 5b shows the peak stress of AZ31 magnesium alloy at different strain rates and temperatures. Similar to yield strength, peak stress decreases with the increase of temperature.

## 2.2 LHGF of AZ31 magnesium bellow with non-uniform temperature field

### 2.2.1 Principle of LHGF with non-uniform temperature field

Long axis magnesium alloy bellow has repetitive elements. If it is formed integrally in one step, extremely large forming dies will be needed. On the one hand, the extremely large forming dies will be very costly, and it also has not only high requirement for the working space but also the clamping force of the hydraulic machine. On the other hand, the AZ31 magnesium alloy needs to be formed at elevated temperature due to the poor formability at room temperature, and lots of energy will be consumed to heat the extremely large forming dies, which will increase the cost of the product significantly. To solve the above problems, local hot gas forming with non-uniform temperature field was proposed in this study to realize the forming of long axis bellow with small dies.

The forming principle of the long axis bellow is shown in Fig. 6. When the temperature of the die in the forming zone reaches the predetermined value, the initial tube blank is positioned in the die. After the tube reaches the forming temperature, the high-pressure gas is introduced into the tube and the first wave is formed. When it is finished, then open the die, move the tube by a wave distance to form the second wave, so as to form all the other waves. In order to avoid the heat effect on the microstructure of the formed waves, the forming die is divided into forming zone with high temperature and cooling zone with low temperature. The cooling zone can also prevent the possible heat damage on the seal ring. The formed wave will not be deformed again in the cooling zone because of the higher yield strength than the materials in the forming zone. It should be noted that only one wave is formed during the forming tests in Section 2.2.2 and 2.2.3 to study the effects

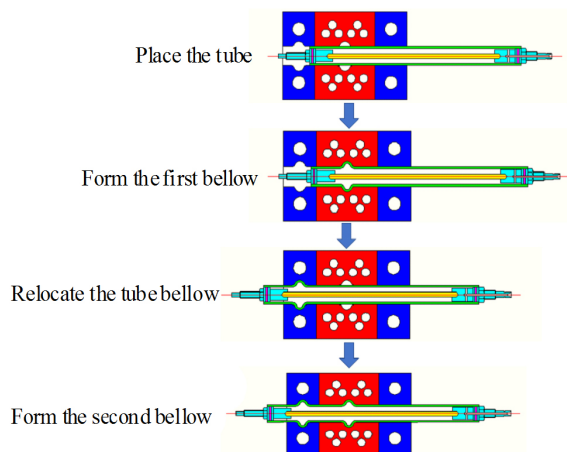


Fig.6 Schematic diagram of the long axis bellow forming process

of forming parameters on the formed part.

### 2.2.2 Effect of temperature on LHGF

In order to investigate the influence of temperature on LHGF, the bellows were formed at 573, 623, 648, and 673 K under the constant gas pressure of 14 MPa, and the bulging height curve of bellows with time is shown in Fig.7. At 573 K, the bellows cannot be fully formed within 1500 s under 14 MPa pressure, and the corresponding maximum height of the bellows is 3.186 mm. When the temperature is higher than 573 K, the bellows can be well formed, but the forming time decreases from 807 s at 623 K to 205 s at 673 K, indicating that temperature has a great influence on forming time.

This is because the flow stress of the material is different under different temperature conditions. The flow stress of the alloy decreases with the increase of temperature. When the gas pressure is constant, the decrease of the flow stress causes the material to deform at a faster rate and leads to a higher forming efficiency.

In order to analyze the influence of temperature on the thickness of the formed parts, the axial thickness of the bellows formed at different temperatures with the same forming pressure of 14 MPa was measured. The distribution of the thinning ratio is shown in Fig.8. Due to the insufficient forming height of bellows formed at 573 K, it is not considered. The selection of measurement points is also shown in Fig.8, where only half of the formed waves are presented with 12 measurement points. Among them, points 1~4 are from the straight wall section, points 5~8 from the transition section, and points 9~12 from the top wave section. The transition section and the top wave section are the forming area.

There are two peak points from points 1 to 12, which are point 7 and point 12. Point 7 is in the transition section and point 12 is in the top of the wave. At 673 K, the maximum thinning ratio is 34.94%, the thinning ratio of the highest point of wave is 28.65%, and the minimum forming thinning ratio is 16.63%, indicating that the thickness distribution is very uneven; at 648 K, the maximum thinning ratio is 35.49%, and the thinning ratio of the highest point of wave is 23.70%; at 623 K, the maximum thinning ratio is 31.69%, the thinning ratio of the highest point of wave is 24.62%, and the minimum thinning ratio of the

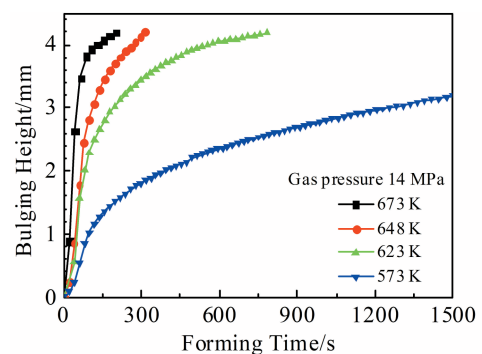


Fig.7 Curves of bulging height with time during the forming at different temperatures

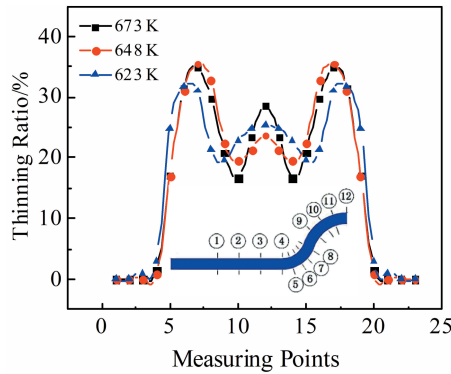


Fig.8 Thickness distribution of bellows formed at different temperatures with a constant gas pressure of 14 MPa

forming area is 19.63%. The uniformity of the thickness distribution increases with decreasing the temperature.

The effect of temperature on the thickness distribution of formed parts is partially because of the different degrees of DRX at different temperatures under the same strain condition. The critical strain required for recrystallization decreases with increasing the temperature. The increasing temperature is helpful to the movement of atoms and can accelerate the migration rate of the grain boundary, leading to more DRX. The dislocation density of the material decreases

because of DRX, and the grain size will also be refined, resulting in the decrease of flow stress. The material softening during LHGF causes the local thinning. Therefore, reducing the forming temperature can improve the uniformity of the thickness distribution after LHGF.

2.2.3 Effect of gas pressure on LHGF

In order to study the effect of gas pressure on the forming results, forming tests with different gas pressure at 673 K were performed, and the loading path and bulging height curves are shown in Fig.9. Three constant gas pressure values of 10, 12 and 14 MPa were selected. The forming time increases from 206 s to 495 s with decreasing the gas pressure from 14 MPa to 10 MPa, indicating that the gas pressure has a significant effect on the forming efficiency.

The strain rate can be calculated according to the bulging height curve, as shown in Fig.10. The increasing gas pressure will increase the strain rate and decrease the forming time. The strain rate increases firstly to a peak value and then decreases gradually until the forming is completed. It can also be seen that the strain rate increases with the increase of gas pressure in the loading stage. After reaching the holding stage, the strain rate decreases continuously. In the later stage of forming, the strain rate remains almost unchanged with value close to 0, indicating that the forming is completed.

Fig. 11 shows the thickness distribution of bellows formed at 648 K with different gas pressures. The overall distribution

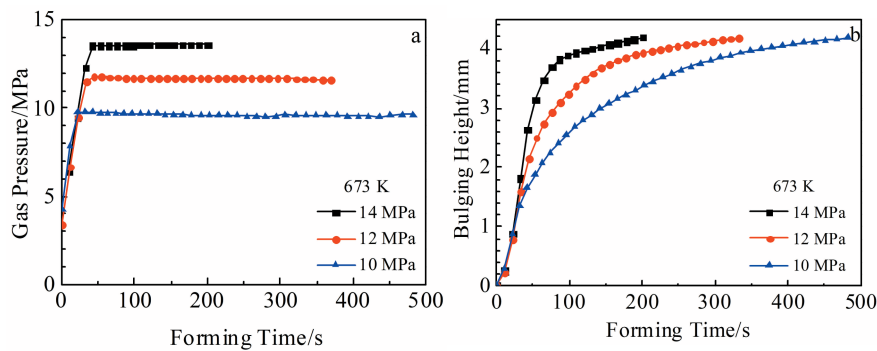


Fig.9 Different gas pressure (a) and bulging height curves (b) during LHGF of bellows at 673 K

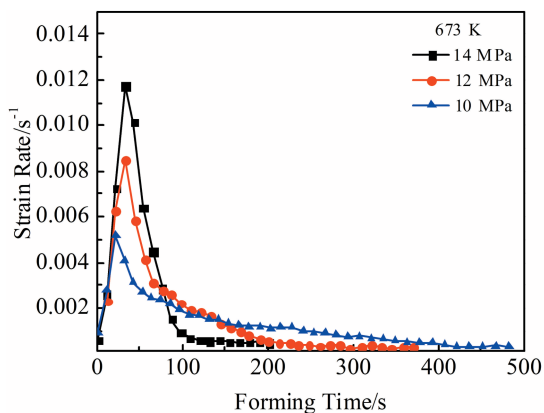


Fig.10 Strain rate distribution during LHGF of bellows at 673 K

is the same as that formed at different temperatures. The maximum thinning points of bellows are all located in the middle of transition section. The top of bellows also has lots of thinning. The maximum thinning ratio decreases from 35.49% to 27.83% as the gas pressure decreases from 14 to 10 MPa. When the gas pressure is 10 MPa, there is a small amount of thickness reduction in the straight wall section (1~4 points), indicating that a small amount of self-feeding occurs during the bulging process, which decreases the overall thinning and increases the thickness uniformity. The self-feeding is affected by the friction. Lower pressure can decrease the friction force and is more conducive to self-feeding, which can improve the uniformity of the thickness distribution.

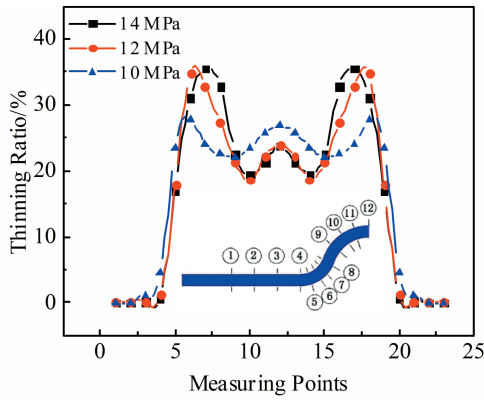


Fig.11 Thickness distribution of bellows formed at 648 K with different pressures

2.2.4 Validation of LHGF and the post-formed microstructure

A long axis bellow with 5 waves is finally formed based on the above investigation; the forming temperature is 623 K and the forming pressure is 14 MPa. During the forming of the long axis bellow, only two waves are in the die cavity, and the other formed waves and undeformed tube are in air with gas pressure inside, so the forming pressure should be selected carefully to avoid the further deformation of the formed wave. Before the final forming, pressure resistance tests of the original tube and the formed bellow with only one wave are carried out at room temperature to determine the proper gas pressure. It is found that the radius of the tube increases by 0.01 mm when the tube is sealed for 300 s at 15 MPa, so it is safe to form the long axis bellow with small dies when the gas pressure is kept below 15 MPa. The final formed part is shown

in Fig.12, and the five waves are accurately formed.

In order to investigate the microstructure of the formed part, the microstructure observation was performed on the highest point A of the bellow, point B in the transition section with great thinning ratio and point D in the undeformed zone. The positions of point A, B and D in the bellows are shown in Fig.13.

Fig. 14 shows the microstructure of the part formed at 623 K. It can be seen that compared with the initial material, the average grain size of point D in the undeformed zone grows from 21.8  $\mu\text{m}$  to 34.7  $\mu\text{m}$  after forming, and some small recrystallized grains are also observed along the grain boundaries, demonstrating that static recrystallization occurs in the straight wall section because of the lack of deformation. Complete DRX occurs at position A, and size of most of the grains ranges from 10  $\mu\text{m}$  to 20  $\mu\text{m}$ , and the overall sample has an average grain size of 16.56  $\mu\text{m}$ . Similar DRX is also



Fig.12 Formed magnesium alloy long axis bellow part

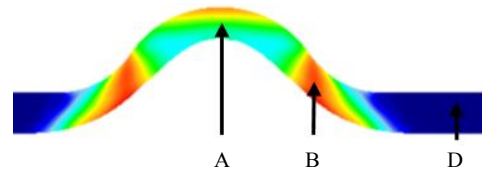


Fig.13 Positions of point A, B and D in the bellow

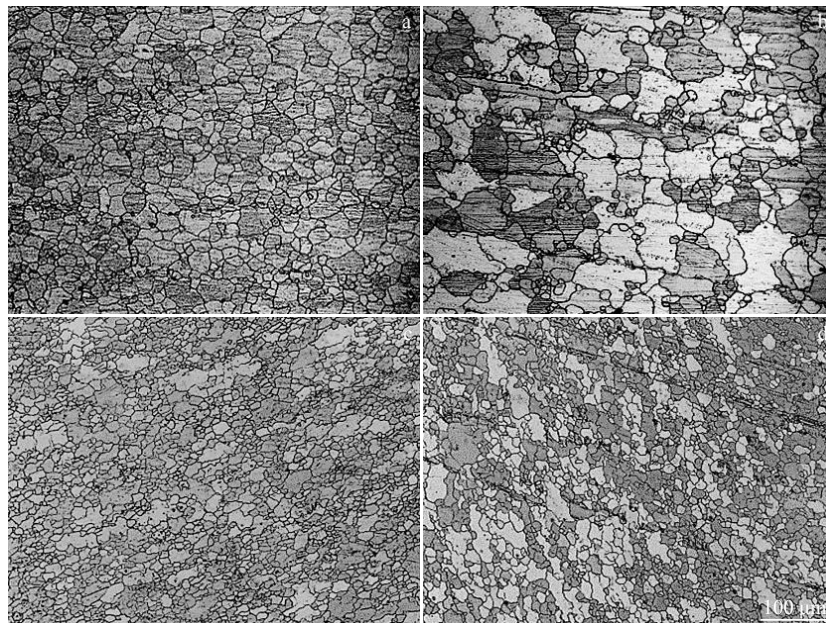


Fig.14 Microstructures in different positions of the bellow formed at 623 K: (a) original structure, (b) point D, (c) point A, and (d) point B

observed in position B, and the average grain size is 15.82  $\mu\text{m}$ , which is smaller than that in position A, because the strain of point B is slightly larger than that of point A. It can be concluded that the microstructure of the deformed part is refined after LHGF, but the grains in the partial area of the straight wall section become coarser after forming. In order to lessen the grain growth in the straight wall section, the length of dies in the forming zone can be reduced to decrease the temperature in the straight wall section and reducing both the soaking and forming time can also be helpful.

### 3 Conclusions

1) A novel local hot gas forming process with non-uniform temperature field is studied by uniaxial tensile tests and forming tests at temperatures ranging from 573 K to 673 K. The effects of temperature and gas pressure on the forming process are explored by forming tests of bellow with one wave under different conditions.

2) The elongation increases with increasing the temperature and decreasing the strain rate, but flow stress decreases. The middle area in the transition section has the largest thinning ratio because of the biaxial tension stress state. The uniformity of the thickness distribution increases with decreasing the temperature due to more material softening at higher temperatures caused by DRX. Lower gas pressure can decrease the friction force and is more conducive to self-feeding, which can improve the uniformity of the thickness distribution.

3) A qualified AZ31 magnesium alloy long axis bellow with 5 waves can be successfully formed with small dies at 623 K under a constant gas pressure of 14 MPa. The average grain size at the wave crest is refined from 21.8  $\mu\text{m}$  in the initial to 16.56  $\mu\text{m}$  after forming, but the average grain size in the straight wall section grows from 21.8  $\mu\text{m}$  to 34.7  $\mu\text{m}$  after forming. Reducing the length of dies in the forming zone and reducing both the soaking and forming time can also be helpful to lessen the grain growth in the straight wall section.

### References

- 1 Hashemi R, Faraji G, Abrinia K et al. *International Journal of Advanced Manufacturing Technology*[J], 2009, 46: 551
- 2 Lee S W. *J Mater Process Tech*[J], 2002, 130-131: 47
- 3 Furushima T, Hung N Q, Manabe K I et al. *J Mater Process Tech* [J], 2013, 213: 1406
- 4 Zhang Z C, Manabe K, Furushima T et al. *Advanced Materials Research*[J], 2014, 936: 1742
- 5 Liu J, Liu Y, Li L et al. *International Journal of Advanced Manufacturing Technology*[J], 2017, 93: 1605
- 6 Kang B H, Lee M Y, Shon S M et al. *J Mater Process Tech*[J], 2007, 194: 1
- 7 Faraji G, Hashemi R, Mashhadi M M et al. *Mater Manuf Process* [J], 2010, 25: 1413
- 8 Liu J, Li H, Liu Y et al. *International Journal of Advanced Manufacturing Technology*[J], 2018, 98: 505
- 9 Hashemi R. *Engineering Solid Mechanics*[J], 2014, 2: 73
- 10 Zheng K, Zheng J, He Z et al. *International Journal of Lightweight Materials and Manufacture*[J], 2019, 3(1): 1
- 11 Dykstra B. *Foreign Locomotive & Rolling Stock Technology*[J], 2002, 6: 12
- 12 He Z B, Teng B, Che C et al. *T Nonferr Metal Soc*[J], 2012, 22: 479
- 13 Yi L, Wu X. *Journal of Materials Engineering & Performance* [J], 2007, 16: 354
- 14 Paul A, Strano M. *J Mater Process Tech*[J], 2016, 228: 160
- 15 Reuther F, Mosel A, Freytag P et al. *Procedia Manufacturing*[J], 2019, 27: 112
- 16 Mosel A, Lambarri J, Degenkolb L et al. *The 21st International ESAFORM Conference on Material Forming*[C]. Palermo: AIP Publishing, 2018
- 17 Rajaei M, Hosseinipour S J, Aval H J. *International Journal of Advanced Manufacturing Technology*[J], 2019, 101: 2609
- 18 Zhubin H E, Fan X, Shao F et al. *T Nonferr Metal Soc*[J], 2012, 22: 364
- 19 Maeno T, Mori K I, Unou C. *Procedia Engineering*[J], 2014, 81: 2237
- 20 Yang J, Wang G, Zhao T et al. *JOM*[J], 2018, 70: 1118

## 长轴波纹管的差温局部热态气压成形新工艺

祝世强<sup>1,2,3</sup>, 王克环<sup>1,2</sup>, 魏文庭<sup>2</sup>, 刘 钢<sup>1,2</sup>

(1. 哈尔滨工业大学 金属精密热加工国家级重点实验室, 黑龙江 哈尔滨 150001)

(2. 哈尔滨工业大学 材料科学与工程学院, 黑龙江 哈尔滨 150001)

(3. 首都航天机械有限公司, 北京 100076)

**摘要:** 针对 AZ31 镁合金长轴波纹管提出差温局部热态气压成形新工艺。首先在温度范围 573~673 K、应变速率范围 0.001~0.1 s<sup>-1</sup> 条件下对 AZ31 镁合金管材进行了热拉伸实验, 分析了温度、应变速率对其力学性能的影响。设计制造了长轴波纹管差温局部热态气压成形装置, 利用该装置, 通过单波波纹管的热气胀成形研究了成形温度、成形内压对波纹管成形时间、壁厚分布的影响规律, 从而确定最佳成形工艺窗口, 并通过五波长波纹管的成形验证该新工艺的可行性。结果表明, 差温成形过程中, 低温区最高温度不超过 50 °C, 高温区温度可以精确控制, 误差在 ±5 °C 以内。在温度 623 K、恒定气压 14 MPa 条件下, 通过小模具成功成形出五波长轴镁合金波纹管。成形后波峰位置平均晶粒尺寸从 21.8  $\mu\text{m}$  细化到 16.56  $\mu\text{m}$ , 其主要原因为成形过程中发生了动态再结晶。

**关键词:** 长轴波纹管; 热态气压; 局部成形; 差温

**作者简介:** 祝世强, 男, 1978 年生, 博士生, 高级工程师, 哈尔滨工业大学金属精密热加工国家级重点实验室, 黑龙江 哈尔滨 150001, 电话: 0451-86418631, E-mail: hitzsq@126.com